NREL
NATIONAL RENEWABLE ENERGY LABORATORY

Simulated Real-World Energy Impacts of a Thermally Sensitive Powertrain Considering Viscous Losses and Enrichment

Preprint

Eric Wood, Jeff Gonder, and Sean Lopp
National Renewable Energy Laboratory

Forrest Jehlik
Argonne National Laboratory

To be presented at the SAE 2015 World Congress and Exhibition
Detroit, Michigan
April 21–23, 2015

NREL is a national laboratory of the U.S. Department of Energy
Office of Energy Efficiency & Renewable Energy
Operated by the Alliance for Sustainable Energy, LLC

This report is available at no cost from the National Renewable Energy Laboratory (NREL) at www.nrel.gov/publications.

Conference Paper
NREL/CP-5400-63255
February 2015

Contract No. DE-AC36-08GO28308

NOTICE

This report is available at no cost from the National Renewable Energy Laboratory (NREL) at www.nrel.gov/publications.

Available electronically at http://www.osti.gov/scitech

Available for a processing fee to U.S. Department of Energy and its contractors, in paper, from:

U.S. Department of Energy
Office of Scientific and Technical Information
P.O. Box 62
Oak Ridge, TN 37831-0062
phone: 865.576.8401
fax: 865.576.5728
email: mailto:reports@adonis.osti.gov

Available for sale to the public, in paper, from:

U.S. Department of Commerce
National Technical Information Service
5285 Port Royal Road
Springfield, VA 22161
phone: 800.553.6847
fax: 703.605.6900
email: orders@ntis.fedworld.gov
online ordering: http://www.ntis.gov/help/ordermethods.aspx

Cover Photos: (left to right) photo by Pat Corkery, NREL 16416, photo from SunEdison, NREL 17423, photo by Pat Corkery, NREL 16560, photo by Dennis Schroeder, NREL 17613, photo by Dean Armstrong, NREL 17436, photo by Pat Corkery, NREL 17721.

Simulated Real-World Energy Impacts of a Thermally Sensitive Powertrain Considering Viscous Losses and Enrichment

Eric Wood, Jeff Gonder, and Sean Lopp
National Renewable Energy Laboratory

Forrest Jehlik
Argonne National Laboratory

Abstract

It is widely understood that cold ambient temperatures increase vehicle fuel consumption due to heat transfer losses, increased friction (increased viscosity lubricants), and enrichment strategies (accelerated catalyst heating). However, relatively little effort has been dedicated to thoroughly quantifying these impacts across a large set of real world drive cycle data and ambient conditions. This work leverages experimental dynamometer vehicle data collected under various drive cycles and ambient conditions to develop a simplified modeling framework for quantifying thermal effects on vehicle energy consumption. These models are applied over a wide array of real-world usage profiles and typical meteorological data to develop estimates of in-use fuel economy. The paper concludes with a discussion of how this integrated testing/modeling approach may be applied to quantify real-world, off-cycle fuel economy benefits of various technologies.

Introduction

A number of studies have demonstrated large negative impacts on fuel consumption and emissions due to colder ambient temperatures. Fuel enrichment and spark timing adjustments for catalyst light-off strategies, high rates of heat transfer, and non-linear viscosity of engine lubricants combine to negatively affect powertrain and drive cycle efficiency in cooler ambient conditions [1-6]. These effects are also present in hybrid powertrains and may be magnified due to the powertrain operating at lower than optimal temperatures [7-9]. Additionally, regional drive cycle variability plays a large role in overall vehicle efficiency [10]. Together, these factors represent important real-world considerations for powertrain design and efficiency.

In 2012 new light-duty fuel economy standards were set for the North American market. The U.S. Environmental Protection Agency (EPA), National Highway Traffic Safety Administration (NHTSA), California Air Resources Board (CARB), original equipment manufacturers (OEMs), non-government entities, and other stakeholders collaborated to define 2012–2025 national fuel economy and greenhouse gas standards. The program called for a 4%–5% annual improvement in fuel economy with the final car and light-duty truck standard set to 54.5 miles per gallon (mpg) [11-12]. Vehicle manufacturer fleet fuel economy certification for this Corporate Average Fuel Economy (CAFE) regulation is determined via a combination of on- and off-cycle methods. On-cycle certification is evaluated from weighted measured testing results of EPA's test cycles [13]. On-cycle certification can be supplemented with off-cycle credits representing estimated real-world vehicle efficiency not captured by on-cycle testing. The EPA and NHTSA currently recognize three pathways in which technologies can qualify for off-cycle credit:

1) **On-Table –** An OEM gets a predefined credit value for technologies that are included in the credit table.
2) **5-Cycle –** An OEM uses a predefined 5-cycle test methodology to determine credit value.
3) **Alternative Method** – An OEM may develop and justify a test methodology and credit value using real-world data.

The first two pathways are set and standardized. The third pathway, the alternative method, requires the use of real-world data in which OEMs and suppliers can demonstrate the viability of the technology and receive appropriate credit for its implementation. The work presented in this paper may serve as a framework to better understand and assess real-world fuel economy impacts for certain technologies.

The approach outlined in this paper includes experimental vehicle chassis dynamometer tests conducted over a wide range of temperatures and loads, coupled with simplified models developed from the experimental data, that are used to demonstrate real-world economy over a broad range of drive cycles and ambient temperatures. Experimental dynamometer tests were conducted at Argonne National Laboratory (ANL) on a 2011 Ford Fusion (2.5L, 6-speed automatic) over a broad range of temperatures. From this data, simplified response surface methodology [14] and lumped capacitance thermal models were developed to simulate vehicle efficiency. These simplified models were integrated into the National Renewable Energy Laboratory's (NREL) Transportation Secure Data Center (TSDC) [15] and coupled with U.S. typical meteorological data [16]. Goodness of fit statistics for the simplified modeling approach are presented with fleet fuel economy impacts quantified for multiple large combinations of real-world drive cycles and historical ambient conditions.

Approach and Test Setup

Tests were conducted at ANL's Advanced Powertrain Research Facility (APRF) four-wheel-drive dynamometer test cell [17]. This dynamometer test facility is designed to handle light- to medium-duty sized (maximum 6,350 kg) vehicles capable of producing up to 373 kW of wheel power. The test cell is EPA 5-cycle capable with ambient temperature capability from -7°C to +36°C. Additionally, the test cell can go to colder temperatures (for this work -17°C). A vehicle fan located at the front of the test cell provides cooling airflow to the vehicle and its powertrain during testing. The simulation fan is a standard vehicle speed-matching fan that fulfills the test regulations for the SC03 air-conditioning (A/C) test. The cell also contains solar lamps simulating a multitude of solar loading conditions experienced in the real-world environment, with a typical target solar loading of 850 W/m^2 at the base of the windshield and/or rear window. The vehicle is restrained to the dynamometer by a tie-down system. Two posts are bolted to T-slot rails on the floor, each post containing a height-adjustable system to restrain the vehicle and to remove vertical load from the wheels on the dynamometer roll.

The test cell contains emission benches capable of bag measuring the criteria emissions total hydrocarbons, oxides of nitrogen, carbon monoxide, soot, as well as carbon dioxide for cycle fuel economy. Additionally a turbine wheel fuel cart is used to accurately measure fuel. A data acquisition system is integrated that allows for a multitude of controller area network, analog, and digital signals to be collected. All data is collected and time aligned at 10 Hz frequency. The test vehicle and APRF test facility is shown in Figure 1.

Figure 1. 2011 Ford Fusion test vehicle on APRF dynamometer for testing.

The vehicle was extensively instrumented to capture pertinent thermal and energy/power nodes. The engine was instrumented with K-type thermocouples to determine coolant, oil, inlet/exhaust temperature at various locations (exhaust port to pre-, mid-bed, and post-catalyst). Accuracy lies within 5°C below 1250°C of measurement, decreasing to 1.1°C at 100°C. Additional K-type thermocouples were included in the transmission and vehicle interior. A strain based torque measurement system was installed on the engine flex plate and half shafts enabling measurement of engine out, transmission input, and transmission output torques and power levels. For the half shafts, full scale torque measurements were set at 3400 Nm with a maximum static measured error of 0.2%. The flex plate full scale torque was set to 500 Nm with a maximum static measured error of 0.2%. Flow measurements for fuel are calibrated within 1.8% of measured error. Engine speed and transmission gear were recorded via CAN signals. Figure 2 represents the pertinent instrumentation and nodes completed for the work.

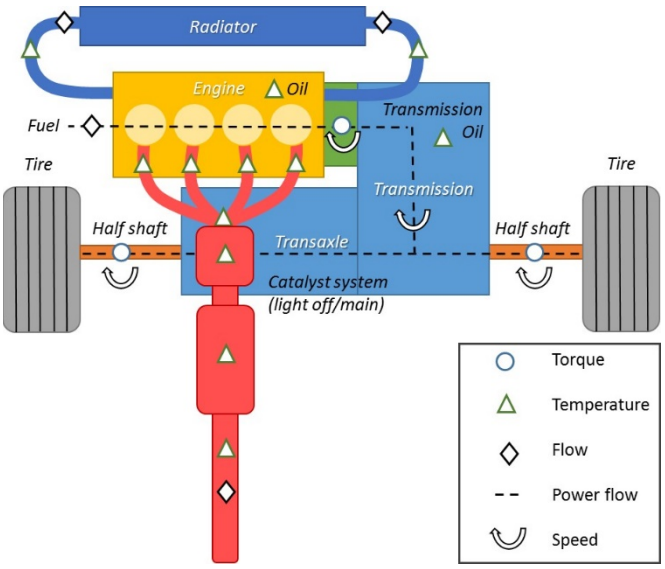

Figure 2. Test vehicle instrumentation layout

To minimize the number of tests completed while maximizing data fidelity, speed/load data from the vehicle was analyzed over the Urban Dynamometer Driving Schedule (UDDS), the Highway Fuel Economy Test (HWFET), and the aggressive US06 cycle. These tests were conducted at +20°C. Both the drive cycle velocities and engine speeds/loads are shown in Figure 4. By comparing the engine loading over the cycles it was determined that testing the vehicle using only the UDDS and US06 cycles would be sufficient in gathering a broad speed/load range, with the HWFET cycle speed/load ranges overlapping the other two cycles, therefore deemed unnecessary.

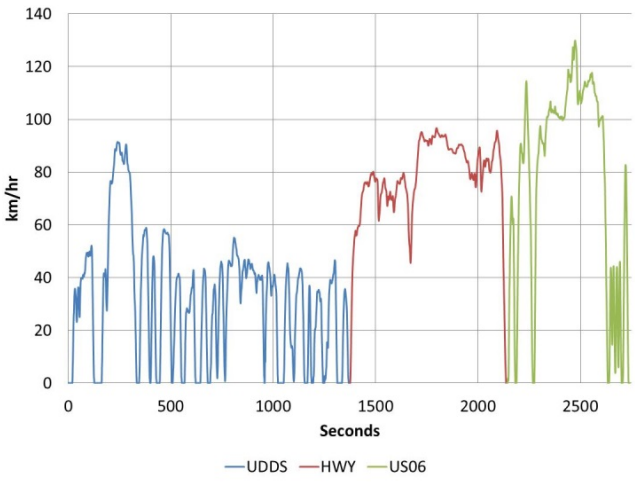

Figure 3. 2011 Ford Fusion velocity profile over the UDDS, HWFET, and US06 cycles.

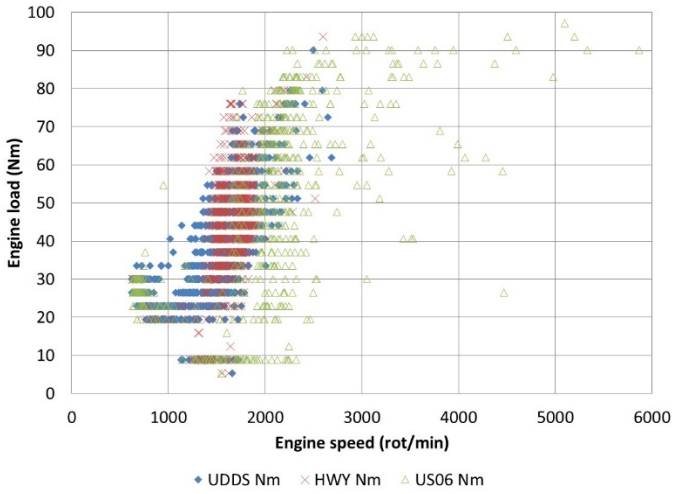

Figure 4. 2011 Ford Fusion engine speed/load points over the UDDS, HWFET, and US06 cycles.

In addition to a wide range of driving behavior, the scope of the work required a broad sweep of thermal conditions for assessment. Both the UDDS and US06 cycles were tested at ambient conditions ranging from -17°C to +35°C. Each of these cycles was tested from cold and hot start conditions. Here, a cold start is defined as the vehicle soaking overnight at the test cell temperature. This allowed for data at cooler powertrain operating states to be collected for both high and low power levels. For hotter tests, the vehicle air conditioner was not used so that the powertrain thermal effects would not be masked by the increased A/C compressor load. For cold tests, the vehicle heater was used and set on the median level. After the dynamometer test, cool-down data were recorded to determine the rate at which the coolant and lubricants cooled following peak operational temperature. Note that additional tests were conducted with the heater in the "on" and "off" positions, and no significant measurable load difference was recorded. Solar loading was not included in the testing as this has no impact on the component efficiency at a components given operational temperature (note: solar loading does, however, increases the rate of component warming thus impacts cycle efficiency). Table 1 lists the final testing matrix.

Table 1. Matrix of test conditions run at APRF (16 tests in total).

Drive Cycle	UDDSx2, US06x2, non-operational cool down
Start Condition	Hot Start, Cold Start
Test Cell Temperature	-17°C, -7°C, +22°C, +35°C

Results

Figures 5 and 6 contrast measured engine oil temperature and integrated cycle fuel consumption over two repetitions of the UDDS drive cycle with the test cell ambient temperature ranging from -17°C to +35°C. As shown, the oil temperature rises from the initial ambient cold-start temperature during the cycle to the final steady state powertrain operational temperature. At -17°C, the engine oil steady state temperature is approximately 18°C cooler than the steady state temperature achieved at +35°C ambient. This is due to the increased convective heat transfer from the powertrain at cooler temperatures. These data are indicative of the results seen for the higher-load US06 cycle (not shown for sake of brevity).

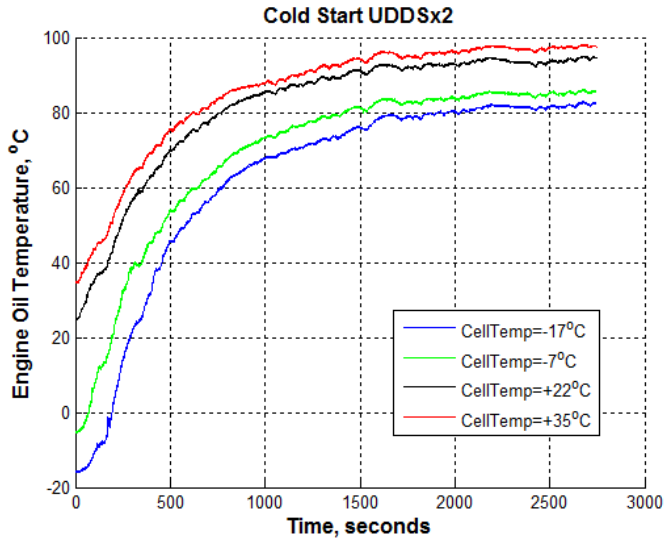

Figure 5. Engine oil warm-up temperatures (measured at dipstick) over two consecutive UDDS cycles following soak to four distinct ambient conditions.

Comparing these results in Figure 6, a significant variation in fuel consumption relative to the temperatures is evident. The increase in fuel consumption for the cold start UDDS cycle at -17°C relative to the +35°C cold start is approximately 22%. Although considered relatively warm, a 3% fuel consumption decrease at +20°C relative to the +35°C UDDS test exists. These results further demonstrate the importance of understanding the real-world thermal effects on vehicle efficiency. This would assist in quantifying the effect that engineering solutions to reduce thermal losses could have on increasing vehicle efficiency.

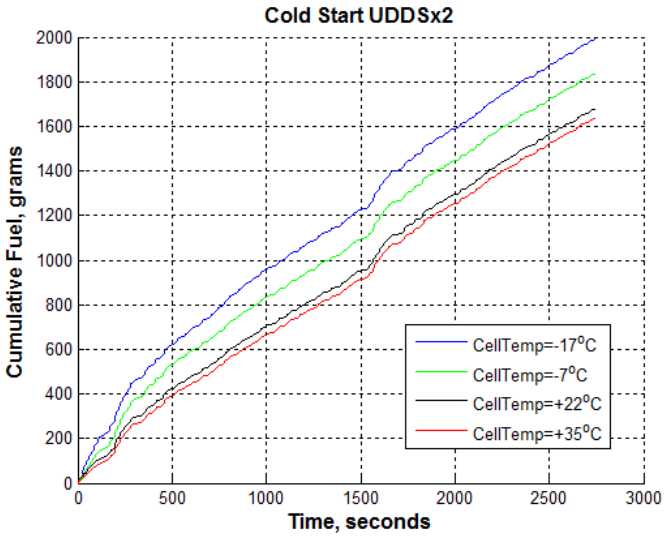

Figure 6. Cumulative fuel use over two consecutive UDDS cycles following soak to four distinct ambient conditions.

Component Model Development

While many modeling approaches exist to estimate vehicle efficiency relative to road loads and powertrain component efficiency, less effort has been expended characterizing the efficiency of internal combustion engines with respect to thermal state. The focus of this work centered on developing a simplified methodology to understand thermal effects in real-world driving conditions without using overly complex models dependent upon accurate measurement of comprehensive component data. Not only are such data not generally available, but simulation of hundreds of thousands of real-world drive cycles from around the country using an unnecessarily complex model would currently be computationally intensive.

The following simplified component models provide a means for predicting component warm-up times and steady-state operating points sensitive to ambient conditions. The generalized approach involves response surface methodology models coupled with simplified lumped capacitance parameter-based models. Application of the Nelder-Mead non-linear optimization method solves for the unknown coefficients to minimize model error relative to vehicle measured results of fuel consumption over the drive cycles and thermal conditions listed in Table 1.

Engine Efficiency

A simplified model of the engine fueling rate as a function of engine power, engine oil temperature, and catalyst light-off was developed. The engine fueling rate is described by a third-order function response surface model with engine output power and engine oil temperature as model inputs[2]. The oil temperature in this case is a differential between the nominal operating temperature and the current oil temperature. The catalyst model is a simplified exponential decay equation that takes into consideration the catalyst temperature until light-off. This equation adds a decaying amount of fuel until a certain catalyst temperature is reached. The engine fueling equations are shown here for reference:

$$fuel = f_1(P_{out}, T_{oil}) + f_2(T_{cat}) \quad (1)$$

$$f_1(P_{out}, T_{oil}) = a_0 + a_{1,1}{P_{out}}^3 + a_{1,2}{P_{out}}^2 + a_{1,3}P_{out} + a_{2,1}{dT_{oil}}^3 + a_{2,2}{dT_{oil}}^2 + a_{2,3}dT_{oil} + a_{3,1}{P_{out}}^3\,{dT_{oil}}^3 + a_{3,2}{P_{out}}^2\,{dT_{oil}}^2 + a_{3,3}P_{out}dT_{oil} \quad (2)$$

$$f_2(T_{cat}) = max(0, a_1 * (e^{a_2*(T_{cat}-a_3)} - 1)) \quad (3)$$

$$dT_{oil} = T_0 - T_{oil} \quad (4)$$

Following the Nelder-Mead solution of the coefficients, plots of the engine efficiency as a function of the engine oil temperature and power output were generated, as well as the time-based comparison between the model's predicted fuel flow and the actual measured data. As an example of the time-based comparison, Figure 7 shows results for a 250-second UDDS cycle segment conducted at -17°C. As these results show, the model matches relatively well with the actual fuel flow measurements recorded during testing.

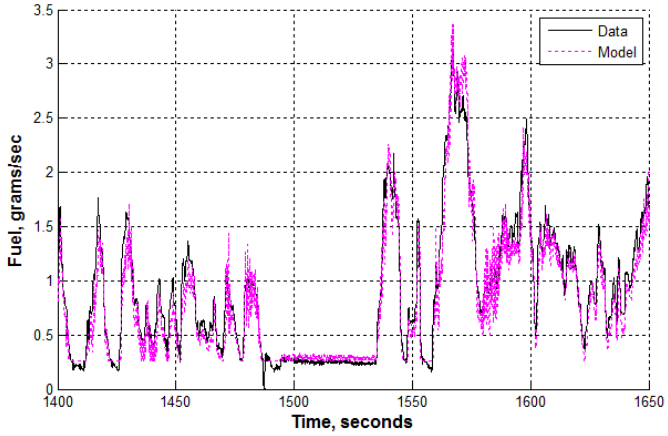

Figure 7. Example time series data of engine fueling rate (250-second section of UDDS). Measured test data from chassis dynamometer (solid black) overlaid with model estimate (dashed magenta).

Figure 8 contrasts the significant impact engine lubricant temperature has on efficiency. An island of optimal efficiency (approximately 36%) exists at power levels between 80 kW and 110 kW and an oil temperature of 100°C. Yet at identical power levels, as engine oil temperature decreases to -17°C, engine efficiencies fall to between 23%–26%, an approximate 33% decrease in overall efficiency for identical power outputs. This underscores the tremendous effect decreased ambient temperatures play on heat engine efficiency.

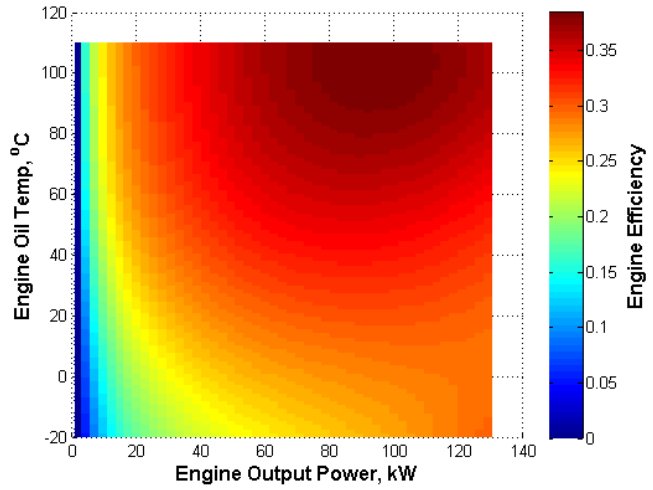

Figure 8. Optimized engine efficiency map as function of output mechanical power and engine oil temperature (considering operation over 16 test cycles).

These results may be best understood by noting the temperature effect on lubricant oil viscosity. Plotting the kinematic viscosity of unused engine oil versus temperature shown in Figure 9 [18], the strong non-linearity of viscosity relative to temperature indicates the excessive friction forces at lower temperatures for the engine. Similar results would be observed for transmission and gear oil as well.

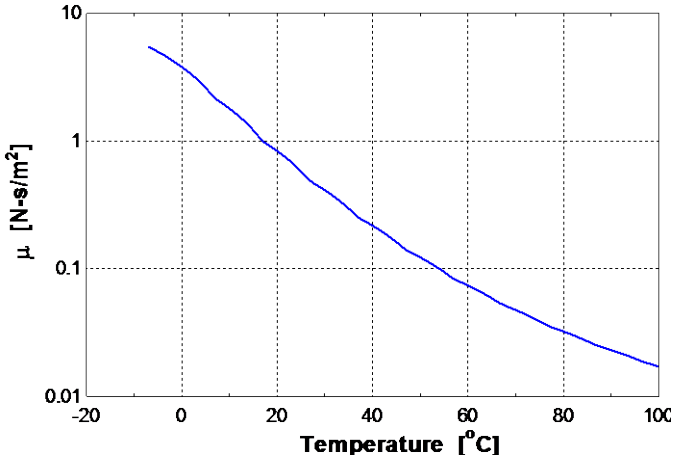

Figure 9. Kinematic viscosity of engine oil as a function of temperature. Note logarithmic viscosity scale. Data taken from EES (engine-oil unused) [18].

Finally, calculations were performed to determine the relative accuracy of the simplified models to predict overall drive cycle fuel consumption for the various drive cycles and temperatures used to develop the model. The results listed in Table 2 show that the maximum predicted deviation from the measured results is 5.2%. The average cumulative error from the measured results of all the cycles is 2.2%, which falls within the range of experimental cycle-to-cycle dynamometer test uncertainty (typically within 3% for a given drive cycle [19]).

Table 2. Cumulative fuel error between measured test data and model estimate (positive error indicates model overestimation).

	UDDS		US06	
Ambient Temp	**Cold Start**	**Hot Start**	**Cold Start**	**Hot Start**
-17°C	-3.9%	1.5%	-5.0%	2.5%
-7°C	0.5%	1.9%	2.5%	5.2%
+22°C	-1.7%	-1.3%	-0.5%	-0.9%
+35°C	-4.1%	-2.0%	-0.5%	-2.8%

Engine Oil Temperature

A simplified lumped capacitance model of engine oil temperature was developed, the parameters of which were fit to the experimental data. The model includes convective heat transfer from the oil to environment, convective transfer between the oil and coolant, and the difference between the power in (fuel mass flow rate) and power out (engine brake torque and speed) of the engine. Additionally, the convective heat transfer term for the engine oil includes a vehicle velocity based function to reflect forced convection as the vehicle velocity increases. This methodology greatly simplifies the process while resulting in accurate estimations. The equations and relative predicted model accuracy are shown below and in Figure 10.

$$\dot{T}_{oil} = \frac{h_1(T_{amb}-T_{oil})+h_2(T_{cool}-T_{oil})+\alpha(P_{out}-P_{in})}{m_{oil}} \quad (5)$$

$$h_1 = a_1 v_{veh} + a_2 \quad (6)$$

Where:

$a_x = Lumped\ coefficents\ to\ solve\ for$

$h_x = Lumped\ convective\ heat\ trasnfer\ coefficients$

$m_{oil} = Mass\ of\ enigne\ oil$

$P_{in} = Power\ into\ engine\ (fuel\ rate\ lower\ heating\ value)$

$P_{out} = Power\ out\ of\ engine\ (brake\ power)$

$T_{amb} = Ambient\ temperature$

$T_{cool} = Coolant\ temperature$

$T_{oil} = Engine\ oil\ temperature$

$v_{veh} = Vehicle\ velocity$

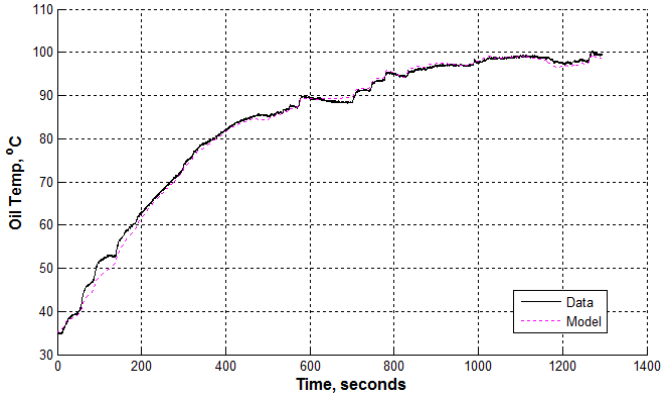

Figure 10. Example time series data of engine oil temperature (measured at dipstick). Measured test data from chassis dynamometer (solid black) overlaid with model estimate (dashed magenta).

Additionally, root mean square error analysis of the instantaneous model-predicted engine oil and actual measured temperature was completed. The results of this analysis (listed in Table 3) show that the average of the instantaneous root mean square error deviation from the actual temperature is 5.3°C. (For reference, the nominal engine oil operating temperature is approximately +100°C). These deviations do not last the entirety of the simulation, but rather for short durations of the simulated cycle.

Table 3. Root mean square of instantaneous error between measured and model-estimated engine oil temperature. The nominal operating temperature of the engine oil is approximately 100°C.

	UDDS		US06	
Ambient Temp	**Cold Start**	**Hot Start**	**Cold Start**	**Hot Start**
-17°C	5.2°C	7.2°C	5.4°C	2.0°C
-7°C	4.9°C	4.1°C	5.5°C	1.9°C
+22°C	5.7°C	6.1°C	8.5°C	2.5°C
+35°C	6.3°C	8.1°C	6.7°C	4.6°C

Engine Coolant Temperature

Similar to the engine oil model, a simplified lumped capacitance model of engine coolant temperature was developed. This model includes convective heat transfer from the coolant to environment, between the coolant and oil, and (similarly to the oil model) the difference between the power in and power out of the engine. Additionally, a logic operator is included that accounts for the thermostat opening which increases the heat transfer from the coolant to the ambient environment, and accounts for vehicle velocity and forced convective heat transfer. The equations and relative predicted model accuracy are shown below and in Figure 11 (see Equations 5 and 6 for variable definitions).

$$\dot{T}_{cool} = \frac{h_1(T_{amb}-T_{cool})+h_2(T_{oil}-T_{cool})+\alpha(P_{out}-P_{in})}{m_{cool}} \quad (7)$$

$$if\ T_{cool} < T_{set}: h_1 = a_1 v_{veh} + a_2, else: h_1 = a_3 v_{veh} + a_4 \quad (8)$$

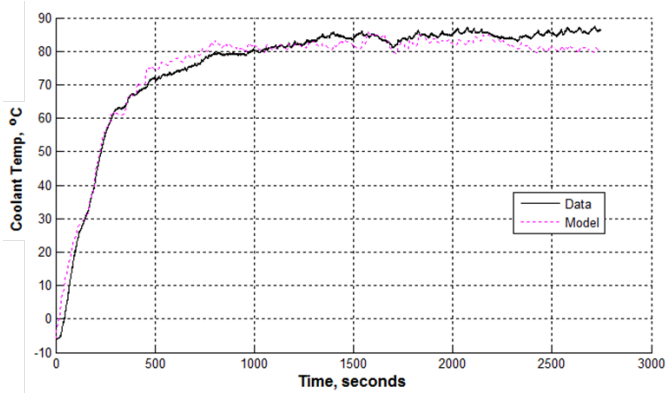

Figure 11. Example time series data of engine coolant temperature (measured at heater core inlet). Measured test data from chassis dynamometer (solid black) overlaid with model estimate (dashed magenta).

Similar to the oil, root mean square error analysis of the instantaneous model coolant and actual measured temperature was completed. The results of this analysis (listed in Table 4) show that the average of the instantaneous root mean square deviation from the actual coolant temperature is 6.9°C. (For reference, the nominal engine coolant operating temperature is approximately +90°C). As was the case for engine oil temperature, these deviations do not last the entirety of the simulation, but rather for short durations of the simulated cycle.

Table 4. Root mean square of instantaneous error between measured and model-estimated engine coolant temperature. The nominal operating temperature of the engine coolant is approximately 90°C.

	UDDS		US06	
Ambient Temp	**Cold Start**	**Hot Start**	**Cold Start**	**Hot Start**
-17°C	7.0°C	9.2°C	7.4°C	3.9°C
-7°C	5.1°C	5.4°C	6.9°C	3.3°C
+22°C	6.8°C	4.3°C	12.5°C	5.9°C
+35°C	6.5°C	6.0°C	10.9°C	9.1°C

Exhaust Catalyst Temperature

The final simplified model is a catalyst thermal model that is used to account for fueling rate enrichment prior to catalyst light off. A simplified lumped capacitance method was applied that included a convective term accounting for heat transfer away from the catalyst to the ambient environment, as well as a fraction of the difference in power between the energy into and out of the engine. As was the case with the coolant and oil, a vehicle velocity term is added to account for forced convection. The equations are listed below, as well as an example of the simultaneous modeled catalyst temperature versus measured results (see Equations 5 and 6 for variable definitions).

$$\dot{T}_{cat} = \frac{h(T_{amb}-T_{cat})+\alpha(P_{out}-P_{in})}{m_{cat}} \quad (9)$$

$$h = a_{h1} v_{veh} + a_{h2} \quad (10)$$

$$\alpha = a_{\alpha 1} T_{cat} + a_{\alpha 2} \quad (11)$$

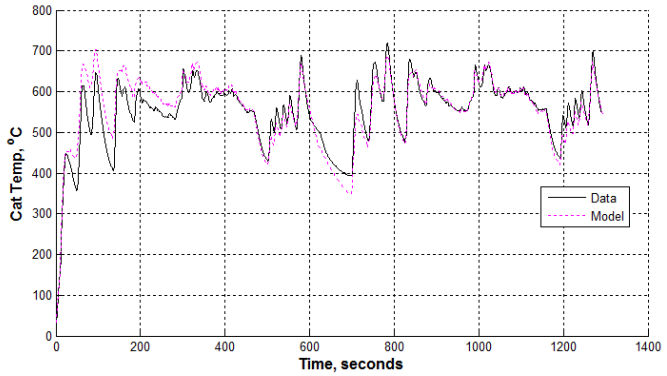

Figure 12. Example time series data of exhaust catalyst temperature (measured pre-catalyst). Measured test data from chassis dynamometer (solid black) overlaid with model estimate (dashed magenta).

As in the case for oil and coolant, instantaneous root mean square error analysis was conducted to determine the relative accuracy of the modeled catalyst temperature against measured results. The results from Table 5 show that the average of the instantaneous root mean square error between the model-predicted and actual temperature is 35.1°C. (For reference, the nominal exhaust catalyst operating temperature is approximately +600°C).

Table 5. Root mean square of instantaneous error between measured and model-estimated exhaust catalyst temperature. The nominal operating temperature of the exhaust catalyst is approximately 600°C.

	UDDS		US06	
Ambient Temp	**Cold Start**	**Hot Start**	**Cold Start**	**Hot Start**
-17°C	69.5°C	26.9°C	70.3°C	24.4°C
-7°C	54.5°C	24.8°C	53.5°C	23.6°C
+22°C	37.5°C	19.8°C	50.1°C	24.6°C
+35°C	34.6°C	20.0°C	38.4°C	24.6°C

Real-World Simulations

Calculation of vehicle road loads in this analysis was performed using NREL's Future Automotive Systems Technology Simulator (FASTSim) [20]. FASTSim is a vehicle simulation tool used to evaluate the impact of various technologies on vehicle performance, cost, and utility in conventional and advanced technology powertrains. FASTSim calculates the power necessary to meet a given speed trace and overcome road loads (rolling, aerodynamic, kinetic, and potential) while considering component limitations, system losses, and auxiliary loads. Given the required engine output power at each time step the engine fuel use is calculated via the thermally sensitive efficiency map as previously detailed, while the differential equations describing the thermal response of engine oil, engine coolant, and exhaust catalyst are evaluated.

Real-world drive cycle data for this study are sourced from the TSDC [15]. Specifically, 1-Hz travel histories one to seven days in duration are queried from vehicles across the United States. These data represent a composite of several data collection efforts from metropolitan planning organizations across the country as documented on the TSDC website (www.nrel.gov/tsdc). Figure 12 shows a geographic distribution of TSDC real-world drive cycle data.

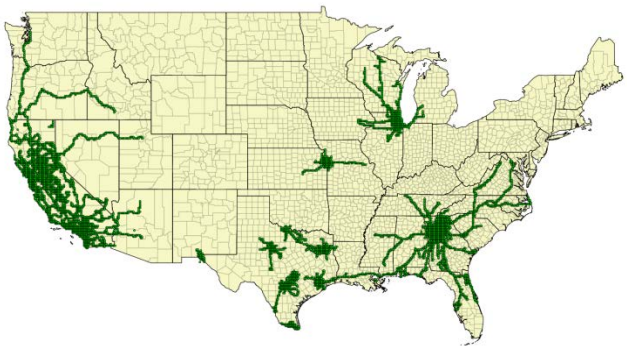

Figure 13. Geographic coverage of 1Hz drive cycle data currently available in the Transportation Secure Data Center (TSDC).

Figure 14 and Figure 15 present real-world trip start and soak time data from the TSDC to inform the frequency of cold-start events and their confluence with daily swings in ambient temperature. A composite of approximately 146,000 trips (consisting of second-by-second speed data) collected across the United States reveals a distribution of trip start times that coincides with traditional traffic patterns (low volumes overnight, a sharp spike in the morning rush hour, a smaller spike around the noon lunch hour, highest volumes around afternoon rush hour, and a slow decline into the evening).

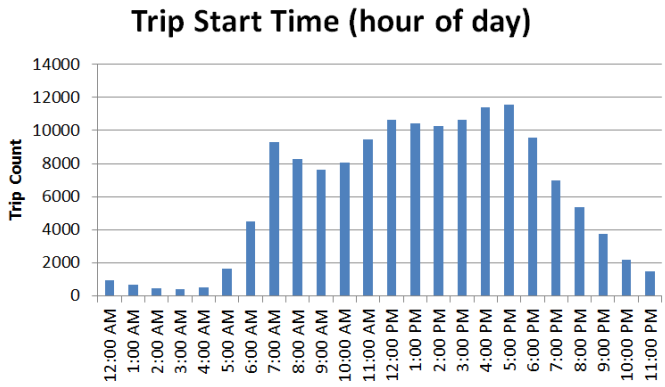

Figure 14. TSDC Trip start-time distribution (by hour of day).

Figure 15 takes the same 146,000 TSDC trips and creates a distribution with respect to soak time (vehicle time in key-off state between trips). Approximately one-third of trips are observed to start following a soak time of greater than four hours; these are trips that can definitively be classified as cold starts. The remaining two-thirds of trips can be thought of as pseudo cold starts given that most engine compartments can be expected to retain some appreciable amount of heat during a park event of this duration. Notably, 20% of trips are observed to start following a soak time of less than 15 minutes. While cold-start effects are generally mitigated by short soak times, these trips represent the greatest potential for thermal retention technologies given the exponential response of passive engine cooling to ambient.

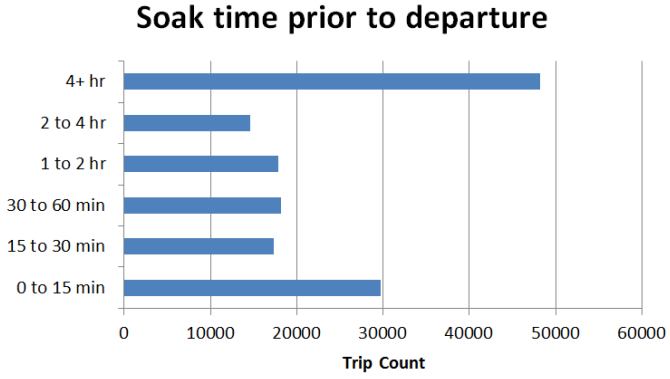

Figure 15. TSDC soak time distribution.

The trip counts presented in Table 6 as a convolution of the data from Figure 14 and Figure 15 reveal the correlation between trip start and soak times. The applied conditional formatting provides a visual sense of trip count magnitudes. For example, the most frequently observed trip starts from the data analysis occur in the 7:00 a.m. hour following a soak of greater than 4 hours (likely the first trip of the day following an overnight soak). Other noteworthy observations include the relatively normal distribution of trips with less than 15 minutes of soak around the 3:00 p.m. hour (potentially characterized by a series of short errand-type trips).

Table 6. TSDC trip counts binned by trip start time and vehicle soak time prior to departure. Conditional formatting applied to express cell values as a color gradient.

		Soak time prior to departure					
		0-15 min	15-30 min	30-60 min	1-2 hr	2-4 hr	4+ hr
Trip Start Time (hour of day)	12:00 AM	169	95	91	82	40	479
	1:00 AM	102	59	69	54	29	339
	2:00 AM	82	30	30	24	21	251
	3:00 AM	44	18	23	13	21	280
	4:00 AM	71	18	36	30	23	346
	5:00 AM	150	45	93	164	93	1103
	6:00 AM	468	149	232	340	283	3031
	7:00 AM	1098	436	574	693	899	5571
	8:00 AM	1281	639	768	985	1133	3460
	9:00 AM	1459	818	987	1145	1017	2187
	10:00 AM	1850	1193	1188	1211	856	1747
	11:00 AM	2200	1364	1627	1356	988	1932
	12:00 PM	2360	1590	1771	1393	1330	2218
	1:00 PM	2304	1602	1520	1398	1480	2127
	2:00 PM	2456	1569	1484	1373	1234	2161
	3:00 PM	2692	1626	1511	1474	1082	2274
	4:00 PM	2612	1570	1642	1501	981	3091
	5:00 PM	2497	1378	1486	1581	1084	3512
	6:00 PM	1857	1109	1152	1371	957	3111
	7:00 PM	1364	825	766	802	518	2724
	8:00 PM	1172	556	524	373	236	2478
	9:00 PM	692	363	284	240	162	1982
	10:00 PM	416	198	157	161	118	1129
	11:00 PM	305	132	116	119	74	716

Ambient temperature data are assembled from NREL's Typical Meteorological Year Database (TMY3) [16]. The TMY3 database contains hourly ambient temperature and solar irradiation data for 1,020 distinct U.S. weather stations. Typical meteorological patterns are synthesized from representative days across historical data from the 1991–2005 timeframe to form a 365-day history with hourly values for each site. Figure 16 shows a map of average yearly ambient temperatures across the continental United States, and Figure 17 shows hourly ambient temperature data from three sample U.S. climates.

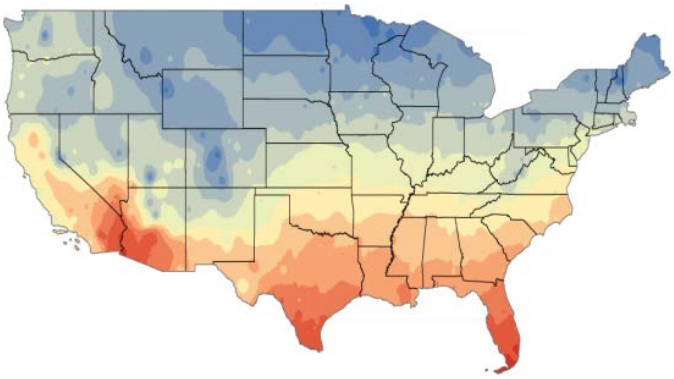

Figure 16. TMY map of average ambient temperatures for the contiguous United States (hot climates in red, cold in blue).

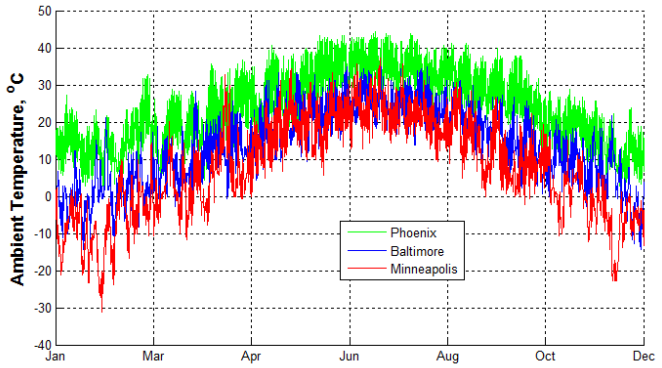

Figure 17. TMY hourly ambient temperature data for Phoenix, Baltimore, and Minneapolis.

By bringing global positioning system travel histories into a shared computing environment with the TMY3 data, it is possible to align real-world drive cycle data with representative ambient temperature data from any major U.S. city at any time of year. This flexibility enables realistic evaluations of simulated vehicle efficiency relative to large amounts of drive cycle and climate data.

Results

Introductory analysis was conducted to investigate the effect ambient temperature has on vehicle fuel consumption when coupled with real-world drive cycle data. As an example, one vehicle from the TSDC data set was selected to demonstrate the effects. Figure 18 shows a time series for this vehicle driving a one-week period from January 2 to January 9 as well as a one-hour magnified trip occurring on January 2.

This figure plots vehicle speed along with oil, coolant and ambient temperatures, and illustrates the modeled response of coolant and oil temperature rise relative to the power requirements of the trip—both the initial rise at the start of each trip segment and the convective cooling period after the vehicle is keyed off. In the modeled response, the coolant temperature rise leads the oil temperature rise (as is the case in the experimental data). Given the relationship between oil temperature and viscosity shown in Figure 9, this means that viscous friction losses would be underestimated during warm-up if engine coolant were instead used as the sole temperature indicator. Additionally, the connection between coolant and engine oil allows the model to capture the increased heat transfer losses as the thermostat opens, reducing the thermal load on the engine oil and thus more accurately predicting the engine thermal state.

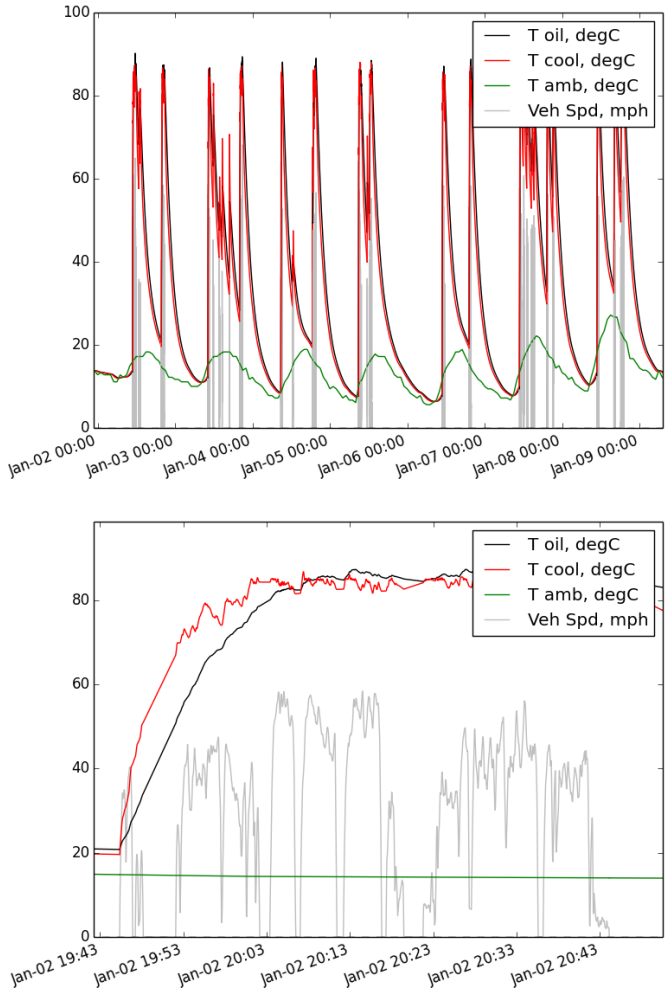

Figure 18. Time series examples of thermal simulations predicting engine oil and coolant temperatures. Real-world drive cycle data overlaid with TMY climate data. Results are show at two horizontal zoom windows: one week (top), and one hour (bottom).

Fleet Statistics

Having established a modeling framework for quantifying real-world efficiency impacts of engine cold-start events, approximately 40 million miles of driving were simulated given combinations of drive cycles (recorded from thousands of U.S. vehicles), local ambient temperature profiles (three representative climates), and weeks of the year (52 in total). Ambient temperature statistics were compiled for U.S. cities from the TMY3 database and climates representing extreme hot and cold scenarios were identified as Phoenix, Arizona and Minneapolis, Minnesota respectively. Ambient temperature data from Baltimore, Maryland were selected as a nationally representative climate scenario.

Figure 19 shows simulation results with distance-weighted, fleet average fuel economy (in miles per gallon of gasoline) plotted by climate and week of year. The first trend identified is the intuitive fluctuation of fuel economy with season. Average fuel economy is shown to decrease by 1–3 mpg during cold winter months as a result of increased viscosity from cooler engine oil temperatures and more frequent fuel enrichment events to accelerate catalyst heating. These are likely conservative estimates of reduced fuel economy during cold weather months, as additional effects including increased transmission oil viscosity, decreased tire pressure, increased air density, and changes in road surface resistance (e.g., snow-covered roads) are not considered in this analysis.

Equally intuitive is the variation between generally hot and cold climates. Simulated Minneapolis fuel economy is shown to be approximately 8% lower during winter months relative to Phoenix, and 2% lower during summer months. In reality, fuel economy during summer months is potentially greater in Minneapolis than in Phoenix, as incremental mechanical loads associated with belt-driven cabin A/C systems have not been included in this analysis.

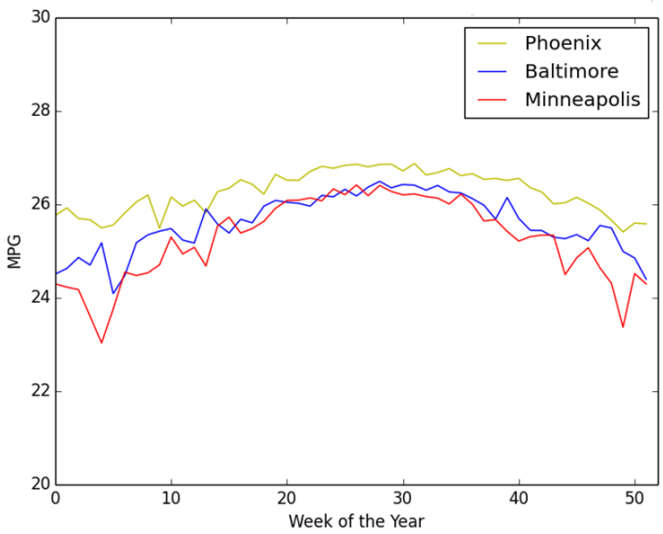

Figure 19. Distance weighted, fleet average miles per gallon by week of year for three U.S. climates.

To highlight variation in fuel economy between drivers, Figure 20 presents efficiency results for all vehicle histories simulated in the Baltimore climate, with individual box plots for each week of the year. In addition to the aforementioned seasonal fuel economy fluctuation, these box plots reveal significant variation between different drive cycle histories with 25th and 75th percentile drivers differing by approximately 5 mpg (~19%). Drive cycle characteristics such as driving speeds, acceleration rates, and percent idle times have been shown to significantly impact simulated fuel economy in previous studies [10]. The featured modeling aspect of this work (engine efficiency sensitivity to thermal state) further exacerbates driver-to-driver fuel economy variation. For example, a driving pattern with several short trips in a week would experience depressed fuel economy as a result of the engine spending a large percentage of operational time under “cold” conditions. These effects are magnified in driving patterns with extended dwell times between trips as components are afforded ample time to decay to ambient temperatures.

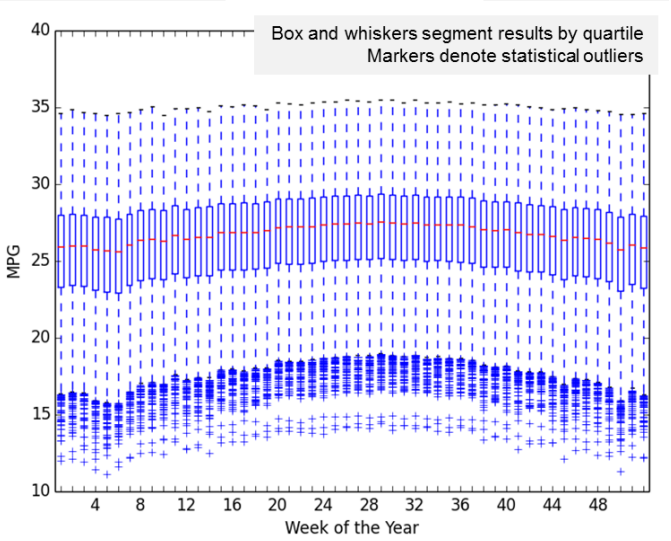

Figure 20. Distribution of simulated vehicle history mpg by week of year (approximately 50% of the data is bounded between 23 and 28 mpg).

Simulated vehicle efficiency data were then aggregated into nine distinct combinations of drive cycle datasets and climate scenarios in Figure 21 to highlight the incremental energy impacts of modeling engine cold starts. The large composite drive cycle data set presented in Figure 19 and Figure 20 is now geographically grouped and anonymously named as drive cycle sets 1, 2, and 3 (statistics for the three aggregated drive cycle datasets can be found in Table 7). The relatively more aggressive drive cycle characteristics of set 3 result in the highest fleet fuel consumption, while set 1 on the whole features less aggressive driving and results in lower fuel consumption. Each of the drive cycle datasets is overlaid with ambient temperature data from the three selected climates with the familiar trends of increased fuel consumption with low average ambient temperature operation.

Figure 21 further shows that the incremental fuel consumption contributions from engine thermal state and enrichment effects account for 4.8% and 2.7% of total simulated fuel use respectively. Taken in aggregate, this is an increase of 7.5% on average and underscores the importance of considering thermal effects in analysis of real-world fuel economy.

Using FASTSim in combination with engine efficiency and thermal models specific to the 2011 Ford Fusion under test, the full EPA 5-cycle test procedure is simulated (including cold FTP and SC03), weighted, and scaled per EPA documentation to determine the modeled vehicle's certification fuel economy. Not surprisingly, the range of simulated real-world fuel consumption values generally falls short of the EPA estimate. This result is likely a byproduct of several real-world effects presently unaccounted for in the modeling environment, including cabin A/C loads and additional powertrain thermal sensitivities (transmission, rear differential, etc.). Accounting for these remaining real-world effects remains a goal of future research.

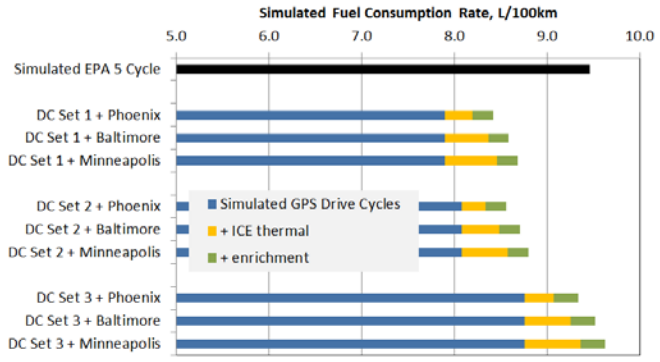

Figure 21. Relative fuel consumption model contributions shown for various combinations of drive cycle datasets and year-long TMY climate data. Results are compared with the simulated EPA 5-cycle test procedure.

Table 7. Distance-weighted drive cycle metrics for the three anonymized sets used in Figure 18.

DC Set	1	2	3
Vehicle Count	413	925	587
Total Miles	16,335	197,400	35,350
Average Driving Speed, mph	39.6	39.2	37.9
Average Positive Acceleration, mph/s	0.762	0.813	0.978

Conclusions

To better understand real-world thermal and driving effects on vehicle efficiency, this effort developed and implemented a novel approach of simplifying experimental data into a predictive model. The approach employed lumped capacitance and response surface modeling methodologies to predict vehicle fuel consumption as a function of velocity and thermal state. The effort focused on developing a simplified, yet accurate, means of predicting vehicle fuel usage over a broad range of drive cycles and ambient temperatures. On average, the simplified model proved able to predict UDDS and US06 fuel consumption in ambient temperatures from -17°C to +35°C to within 2.2% of the actual test measured values.

These simplified models were then run through a large data set of 1-Hz travel histories ranging from one to seven days in duration from vehicles across the United States. Additionally, the models and travel histories were coupled with a typical meteorological year database in order to capture the interplay of real-world driving behavior (speeds, trip times, distances, etc.) with daily and seasonal ambient temperature variation. Using Phoenix, Baltimore, and Minneapolis as regional examples, the effort modeled three different fleet data sets to better understand seasonal and regional fuel consumption differences. The results show significantly higher fuel consumption in the colder Minneapolis climate relative to Phoenix. Average simulated real-world fuel use associated with viscous losses in the engine and fuel enrichment was found to be 7.5%.

As regulated fuel economy standards continue to climb, both in the United States and globally, the ability of certification test procedures to accurately represent on-road vehicle efficiency continues to

increase in importance, especially in the case of emerging technologies. OEMs interested in receiving appropriate credit for technologies with significant off-cycle potential will be tasked with justifying fuel economy claims using large samples of statistically representative data. The integrated testing/modeling approach presented in this paper represents one such potential solution to quantifying real-world fuel economy.

Computational models of vehicle efficiency calibrated on high-resolution laboratory data and evaluated over large databases of driving behavior and typical meteorological conditions provide a controlled process for generating repeatable estimates of on-road fuel economy with reasonable investments of time and effort. While modeling in this study focused on a baseline, conventional vehicle, the methodology can be easily applied to evaluate technologies with potential off-cycle savings (e.g., engine encapsulation, a high-efficiency alternator, or engine start/stop). Analysis over equivalent drive cycle and ambient temperature data would enable direct comparison with the baseline conventional vehicle.

Going forward, the authors intend to build upon the described methods by:

- Incorporating additional model sensitivities to capture transmission thermal efficiency and cabin A/C loads.
- Validating the model's real-world fuel economy estimates to on-road data from an instrumented vehicle.
- Weighting results to generate fuel economy estimates statistically representative of the national fleet based on distributions of available drive cycle data and the location of vehicle populations relative to meteorological data.

References

1. Ostrouchov, N., "Effect of Cold Weather on Motor Vehicle Emissions and Fuel Economy," SAE Technical Paper 780084, 1978, http://papers.sae.org/780084/
2. Jehlik, F., Rask, R., and Christensen, M., "Development of Variable Temperature Brake Specific Fuel Consumption Engine Maps," SAE Technical Paper 2010-01-2181, 2010, http://papers.sae.org/2010-01-2181/
3. Kunze, K., Wolff, S., Lade, I., and Tonhauser, J., "A Systematic Analysis of CO2 Reduction by an Optimized Heat Supply During Vehicle Warm-Up," SAE Technical Paper 2006-01-1450, 2006. http://papers.sae.org/2006-01-1450/
4. Andrews, G.E., Harris, J.R., and Ounzain, A., "SI Engine Warm-Up: Water and Lubricating Oil Temperature Influences," SAE Technical Paper 892103, http://papers.sae.org/892103/
5. Andrews, G.E., Harris, J.R. and Ounzain, A., "Experimental Methods for Investigating the Transient Heating and Emissions of an SI Engine During the Warm-Up Period," in: Experimental Methods in Engine Research and Development, *IMechE*, pp.101-108, 1988.
6. Andrews, G.E., Ounzain, A.M., Li, H., Bell, M., Tate, J., and Ropkins, K., "The Use of a Water/Lube Oil Heat Exchanger and Enhanced Cooling Water Heating to Increase Water and Lube Oil Heating Rates in Passenger Cars for Reduced Fuel Consumption and CO2 Emissions During Cold Start." SAE Technical Paper 2007-01-2067. http://papers.sae.org/2007-01-2067/
7. Carlson, R., Duoba, M., Bocci, D., Lohse-Busch, H., "On-Road Evaluation of Advanced Hybrid Electric Vehicles Over a Wide Range of Ambient Temperatures," Paper #275, EVS23, 2007, http://www.transportation.anl.gov/pdfs/HV/456.pdf
8. Carlson, R., Christenson, M., Shinomiya, R., "Influence of Sub-Freezing Conditions on Fuel Consumption and Emissions of Two Plug-In Hybrid Electric Vehicles," EVS-24, Paper #2760135, 2009.
9. Jehlik, F., "Methodology and Analysis of Determining Plug-In Hybrid Engine Thermal State and Resulting Efficiency," SAE Technical Paper 2009-01-1308, 2009, http://papers.sae.org/2009-01-1308/
10. Neubauer, J., and Wood, E., "Accounting for the Variation of Driver Aggression in the Simulation of Conventional and Advanced Vehicles," SAE Technical Paper 2013-01-1453. http://www.nrel.gov/docs/fy13osti/58609.pdf
11. The White House, Office of the Press Secretary, "Obama Administration Finalizes Historic 54.5 mpg Fuel Efficiency Standards," http://www.whitehouse.gov/the-press-office/2012/08/28/obama-administration-finalizes-historic-545-mpg-fuel-efficiency-standard, accessed November 19, 2014.
12. U.S. Federal Register, Environmental Protection Agency, Department of Transportation, National Highway Traffic Safety Administration "2017 and Later Model Year Light-Duty Vehicle Greenhouse Gas Emissions and Corporate Average Fuel Economy Standards; Final Rule," http://www.gpo.gov/fdsys/pkg/FR-2012-10-15/pdf/2012-21972.pdf, accessed October 1, 2014.
13. U.S. Department of Energy and U.S. Environmental Protection Agency "Fuel Economy Tests: Detailed Test Information," http://www.fueleconomy.gov/feg/fe_test_schedules.shtml, accessed November 19, 2014.
14. Myers, R.H., and Montgomery, D.C., "Response Surface Methodology: Process and Product Optimization Using Designed Experiment," Wiley-Interscience, 1995.
15. "Transportation Secure Data Center." (2013). National Renewable Energy Laboratory. Accessed October 1, 2013: www.nrel.gov/tsdc.
16. National Renewable Energy Laboratory, "National Solar Radiation Database, Typical Meteorological Year Database 3," Golden, CO, http://rredc.nrel.gov/solar/old_data/nsrdb/1991-2005/tmy3/ , accessed July 2011.
17. Argonne National Laboratory, Transportation Technology R&D Center "Advanced Powertrain Research Facility (APRF)," http://www.transportation.anl.gov/facilities/aprf.html, accessed October 1, 2014.
18. Data generated using Engineering Equation Solver (EES), V9.649-3D which contains built in thermodynamic and physical properties of unused engine oil. http://www.fchart.com/ees/
19. "J-2951 Dynamometer Repeatability Testing," ANL internal study, 2013. http://standards.sae.org/j2951_201111/
20. National Renewable Energy Laboratory, "Future Automotive Systems Technology Simulator," www.nrel.gov/fastsim, accessed October 1, 2013.

Contact Information

Advanced Powertrain Research Facility
Argonne National Laboratory
Energy Systems Division
9700 S. Cass Ave.
Argonne, IL 60439

Forrest Jehlik
(630) 252-6403
fjehlik@anl.gov

Transportation and Hydrogen Systems Center
National Renewable Energy Laboratory
15013 Denver West Pkwy MS 1634
Golden, CO 80401

Eric Wood
(303) 275-3290
eric.wood@nrel.gov

Jeffrey Gonder
(303) 275-4462
jeff.gonder@nrel.gov

Sean Lopp
(303) 275-4549
sean.lopp@nrel.gov

Acknowledgments

This study was supported by the U.S. Department of Energy's Vehicle Technologies Office. The authors would specifically like to thank Lee Slezak and David Anderson for their guidance.

In addition to U.S. DOE support, data archiving and processing in the TSDC are also supported by the U.S. Department of Transportation's Federal Highway Administration. The authors would specifically like to thank Elaine Murakami for her guidance and support.

Use of Argonne National Laboratory's Advanced Powertrain Research Facility and the National Renewable Energy Laboratory's FASTSim software (both developed under funding from the U.S. Department of Energy's Vehicle Technologies Office) were critical to the completion of this study. Special thanks to Eric Rask (ANL), Mike Douba (ANL), and Aaron Brooker (NREL).

Definitions/Abbreviations

°C	Degrees centigrade
A/C	Air Conditioning
ANL	Argonne National Laboratory
APRF	Advanced Powertrain Research Facility (ANL)
DOE	U.S. Department of Energy
EPA	U.S. Environmental Protection Agency
FASTSim	Future Automotive Systems Technology Simulator
HWFET	Highway Fuel Economy Test (EPA defined)
Hz	Hertz frequency
mpg	miles per gallon
NHTSA	National Highway Traffic Safety Administration
NREL	National Renewable Energy Laboratory
OEM	Original Equipment Manufacturer
SC03	Supplemental air-conditioning dynamometer test procedure (EPA defined)
TMY	Typical Meteorological Year
TSDC	Transportation Secure Data Center
UDDS	Urban Dynamometer Driving Schedule (EPA defined)
UDDSx2	Back-to-back UDDS driving tests
US06	US06 dynamometer driving schedule (EPA defined)
US06x2	Back-to-back US06 dynamometer driving tests